Journal of Ultrafine Grained and Nanostructured Materials
https://jufgnsm.ut.ac.ir
Vol. 56, No.2, December 2023, pp. 165-172
Print ISSN: 2423-6845 Online ISSN: 2423-6837
DOI: 10.22059/jufgnsm.2023.02.05

Hall-Petch analysis of fine-grained AISI 309Si stainless steel upon recrystallization and grain growth annealing

Kimia Saberi Tavakoli [1], Ata Abdi [2], Mohammad Javad Sohrabi [1], Alireza Kalhor [3], Hamed Mirzadeh *,[1]

[1]School of Metallurgy and Materials Engineering, College of Engineering, University of Tehran, Tehran, Iran,
[2]Faculty of Materials Science and Engineering, K. N. Toosi University of Technology, Tehran, 19395-1999, Iran;
[3]Faculty of Materials Engineering, Silesian University of Technology, Krasińskiego 8, 40-019, Katowice, Poland.

Recieved: 20 November 2023; Accepted: 26 December 2023

**Corresponding author email: hmirzadeh@ut.ac.ir*

ABSTRACT

Hall-Petch analysis and the effect of the average grain size (D) on the hardness (H) of AISI 309Si stainless steel should be systematically investigated. This aim was achieved by cold rolling (reduction of thickness of 90%) followed by annealing at 1000 °C for different holding times. Cold rolling led to the formation of deformation-induced α′-martensite and work-hardening of the retained austenite, which led to an increased hardness of 427 HV compared to the hardness of 115 HV for the as-received sample. X-ray diffraction (XRD) analysis revealed the formation of ~30 vol% martensite, which signifies the higher mechanical stability of austenite in this alloy when compared to the metastable grades. At the annealing temperature of 1000 °C, the material is fully austenitic without any intermetallics. Moreover, by occurrence of martensite reversion, recrystallization of the retained austenite, and subsequent grain growth, it is easy to obtain different grain sizes at this temperature. Annealing at 1000 °C for 30 min resulted in a significant increment of hardness (155.1 HV) compared to the as-received sample as well as the formation of a fine-grained microstructure with an average grain size of 6.7 µm, which is equivalent to ~93% refinement of the grain size. Longer annealing times led to the occurrence of grain growth with the resulting decrement of hardness, where $D-D_0=2.1762\times10^{11}\exp(-280000/RT)\times t^{0.5}$ was proposed to predict the grain size during grain coarsening. Moreover, the Hall–Petch relationship of $H=140.1/\sqrt{D}+100.7$ was proposed for the first time, in which the H_0 value of 100.7 HV was also compared to those determined for AISI 316L (130.0 HV) and 304L (160.4 HV) alloys. Furthermore, it was revealed that the increased metastability leads to an increment in the H_0 value, which can be correlated with the $M_{d30/50}$ temperature.

Keywords: AISI 309Si stainless steel; Strain-induced martensitic transformation; Recrystallization; Hall-Petch analysis.

1. Introduction

AISI 309Si austenitic stainless steel is a heat resistant alloy with high amounts of Cr (19 to 21 wt.%), Ni (11 to 13 wt.%), and Si (1.5 to 2.5 wt.%) in its chemical composition. Due to its excellent corrosion and oxidation resistance, this alloy is widely used in the elevated-temperature applications in chemical plants and for welding, surpassing the performance of common austenitic alloys such as AISI 304L and 316L stainless steels [1,2].

Grain refinement of this alloy is a viable approach to improving mechanical properties due to the grater resistance to dislocation movement as well as the stronger passive film due to the higher grain boundary density [3]. Owing to the presence of high amounts of alloying elements, the austenite phase in the AISI 309Si stainless steel is more stable against strain-induced martensitic transformation compared to the AISI 304L and 316L stainless steels [4]. Therefore, grain refinement of

this alloy via reversion of strain-induced martensite to fine-grained austenite is limited, and hence, thermomechanical processing [5,6] as well as cold rolling followed by recrystallization annealing [7] can be considered the main approach for grain refinement.

There are few reports on the recrystallization as well as the formation of martensite in AISI 309 grade and its reversion during subsequent annealing. Abdi et al. [3] reported that cold rolling led to the formation of strain-induced martensite in the AISI 309Si stainless steel sheets. During subsequent annealing, two regimes of transformations for reversion and recrystallization were identified. These authors were able to propose a recrystallization-temperature-time diagram for phase transformations in this alloy. In another study on the related AISI 309S alloy, Eskandari et al. [1] characterized the optimum annealing temperature and time for achievement of a uniform recrystallized grain size after cold rolling, which resulted in the improvement of mechanical properties. However, there is no report on the effect of grain size and Hall-Petch analysis of AISI 309Si stainless steel. Accordingly, in the present work, this aim was achieved by cold rolling followed by annealing at elevated temperatures. Moreover, the behavior of this alloy was critically discussed and compared to other stainless steels.

2. Experimental material and procedure

Room-temperature cold rolling with the reduction in thickness of 90% based on the multi-pass approach with average reduction in thickness of 10% in each pass was applied to the AISI 309Si stainless steel sheet with the chemical composition shown in Table 1, which was determined by the spark optical emission spectrometry. This material was received in the sheet form with the thickness of 10 mm and it was in the annealed condition with fully austenitic microstructure. Subsequently, annealing at an elevated temperature of 1000 °C for holding times up to 120 min was applied to the cold-rolled sheet with the aim of recrystallization for grain refinement as well as grain growth for obtaining different grain sizes, as schematically shown in Figure 1.

Following electropolishing (H_3PO_4-H_2SO_4 solution, 40 V) [8], electroetching in the $C_2H_2O_4$-H_2O Oxalic acid solution at 4 V [3] was applied to reveal the microstructural features using optical microscopy. Hardness measurements were based on the Vickers hardness test, for which a load of 5 kg and the dwell time of 15 s were applied. Moreover, the average value of five indentations was consid-

Table 1- Chemical composition (wt.%) of the investigated alloy

Alloy	C	Cr	Ni	Si	Mn	Cu	Mo	Fe
309Si	0.05	20.0	11.5	1.9	0.8	0.3	0.3	balance

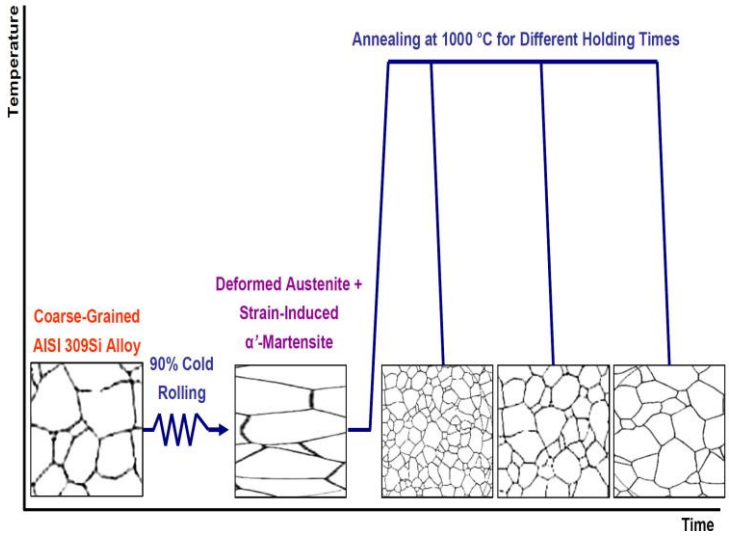

Fig. 1- Schematic illustration of the processing route used in this work, representing the grain refinement achieved by cold rolling and annealing, as well as the subsequent grain growth upon increasing the holding time.

ered for each condition. Phase analysis was based on the X-ray diffraction (XRD) method, for which a PHILIPS PW-3710 with Cu-Kα radiation was used. Based on the important diffraction peaks of α′-martensite and austenite (γ), Equation 1 was used to obtain the martensite fraction, which has been specifically developed to obtain the fraction of α′-martensite in austenitic stainless steels [9-11]:

$$f_{\alpha'} = \frac{I_{(211)\alpha'}}{I_{(211)\alpha'} + 0.65(I_{(311)\gamma} + I_{(220)\gamma})} \quad (1)$$

3. Results and discussion

3.1. As-received and cold-rolled states

The XRD patterns and microstructures of the as-received and cold-rolled samples are depicted in Figure 2. It can be seen that the as-received microstructure has an average grain size of 95 μm. Upon cold rolling, the grains are deformed and elongated, which is related to the effect of plastic deformation at low temperatures that results in the work-hardening of the material. The XRD pattern of the as-received sample reveals the presence of the diffraction peaks of the austenite phase, as expected. Therefore, the as-received sample is completely austenitic. However, after cold rolling, the peaks of the α′-martensite phase have also appeared in the diffraction pattern, which reveals the formation of the strain-induced α′-martensite during rolling at room temperature. Based on Equation 1, the amount of α′-martensite can be determined as 29.7 vol%. The hardness of the cold-rolled sample was promoted to 427 HV from the low value of 115 HV for the as-received sample. This improvement is related to the work-hardening of the retained austenite as well as the formation of α′-martensite. It is well-known that the formation of α′-martensite is an important hardening phenomenon in metastable stainless steels such as AISI 304, 316, and 2205 stainless steels [12,13]. On the other hand, 30 vol% α′-martensite after heavy cold rolling of 90% at room temperature reveals that the austenite phase in AISI 309Si stainless steel is quite stable when compared to the formation of almost completely martensitic microstructure in AISI 304 stainless steel at lower rolling reductions in thickness [14,15]. This can be related to the much higher stacking fault energy (SFE) of the AISI 309Si stainless steel compared to the AISI 304 stainless steel due to the high amounts of alloying elements such as Ni and Cr in the former alloy by consideration of Equation 2 [16]:

$$SFE(mJ/m^2) = -53 + 6.2Ni + 0.7Cr + 3.2Mn + 9.3Mo \quad (2)$$

3.2. Annealed state

Upon annealing at 1000 °C, the preliminary experiments revealed that the cold-rolled sheet will be completely reversed (based on the XRD pattern of Figure 3a) and recrystallized at holding time of 30 min; while at lower holding times, partially recrystallized microstructures were observed. At longer holding times, coarsening of the grain size is resulted by the operation of grain growth phenomenon [17]. Accordingly, the holding times of 30, 45, 60, and 120 min were considered to follow the change in grain size during annealing. The obtained microstructures and the measured average grain sizes are summarized in Figure 3b. It can be seen that the sample annealed for up to 30 min has a fine grain size of 6.7 μm, which reveals a significant grain re-

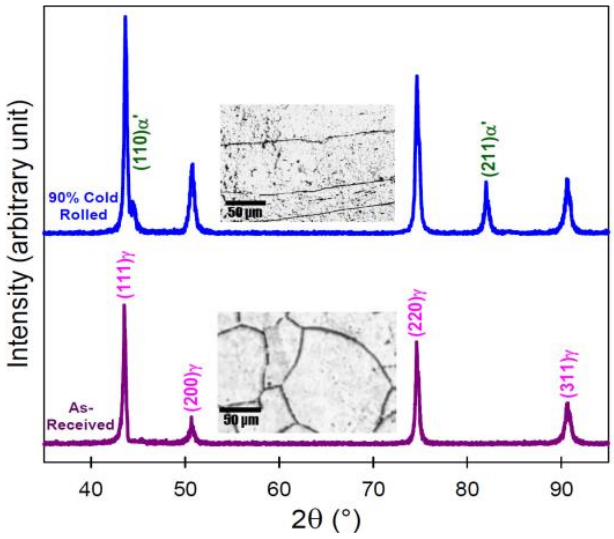

Fig. 2- XRD patterns and the representative microstructures of the as-received and cold-rolled samples.

finement when compared to the average grain size of 95 μm for the as-received sample. This is equivalent to ~93% reduction in the grain size, which can be related to the heavy deformation of 90% and the formation of ~30 vol% α′-martensite in the rolling stage; and the reversion of martensite to austenite [18] as well as the recrystallization of the heavily deformed austenite [19-21] in the annealing stage.

As can be seen in Figure 3b, annealing times longer than 30 min resulted in grain growth. For instance, 120 min annealing at 1000 °C resulted in an average grain size of 14 μm. This is equivalent to ~100% increase in the grain size compared to the recrystallized grain size of 6.7 μm. Anyway, the grain size of 14 μm is still much finer than the initial grain size of 95 μm. Moreover, the parabolic shape of the grain growth curve is evident, which needs to be investigated and quantified.

3.3. Grain growth kinetics

The normal grain growth kinetics can be represented by the following equation [22]:

$$D - D_0 = kt^{1/n} \tag{3}$$

where D is the grain size at time t, D_0 is the initial grain size (here it is equal to the recrystallized grain size of 6.7 μm), n is the grain growth exponent with the theoretical value of 2 [23], and k is a temperature-dependent constant, which can be expressed as follows:

$$k = k_0 \exp(-Q / RT) \tag{4}$$

where T is the annealing temperature, k_0 is the proportionality constant, and Q is the grain growth activation energy with the theoretical value equivalent to the lattice self-diffusion activation energy [24]. According to Equation 3, taking the natural logarithm leads to Equation 5, and based on this equation, the plot of ln(D-D_0) versus lnt can be used to obtain the values of k and n. In fact, the slope of the intercept of this plot gives the values of 1/n and lnk, respectively. The corresponding plot is shown in Figure 4. It can be seen that the slope is 0.4926, and hence, n is 2.03, which is consistent with the theoretical value of 2.

$$\ln(D - D_0) = \ln k + \frac{1}{n} \ln t \tag{5}$$

By consideration of lnk = -0.3497 (based on Figure 4) and the lattice self-diffusion activation energy of 280 kJ/mol for austenite in austenitic stainless steels [25], the following equation can be derived for the kinetics of grain growth in this alloy:

$$D - D_0 = 2.1762 \times 10^{11} \exp(-280000 / RT) \times t^{1/2} \tag{6}$$

where D and t are expressed in μm and min, respectively.

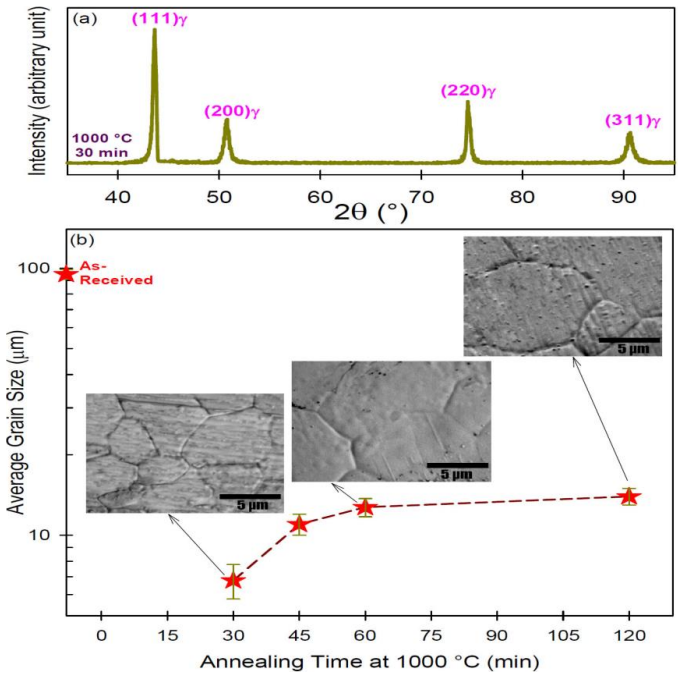

Fig. 3- (a) XRD pattern of the sample annealed at 1000 °C for 30 min, and (b) measured grain sizes and representative microstructures of the annealed samples.

3.4. Evolution of hardness and Hall-Petch analysis

The measured hardness values of annealed samples are depicted in Figure 5. It can be seen that the thermomechanical processing of cold rolling and recrystallization annealing has led to a significant improvement in hardness when compared to the as-received sample. This is related to the remarkable grain refinement, as shown in Figure 3. However, by increasing the annealing time and increasing the grain size due to grain growth, the hardness decreases, as shown in Figure 5. Therefore, there is an inverse relationship between hardness and grain size, which will be treated in the following.

It is well established that the yield stress and/or hardness of metallic materials can be correlated to the inverse root of the average grain size by the Hall-Petch relationship [26-28]. For hardness, the Hall-Petch relationship can be represented as follows:

$$H = H_0 + K/\sqrt{D} \quad (7)$$

where H_0 is the friction stress and K is the locking parameter or Hall-Petch slope, respectively. The corresponding plot is shown in Figure 6. The figure reveals that the data points are consistent with the Hall-Petch line, revealing that the hardness of the alloy can be correlated to its average grain size according to the following equation:

$$H(\mathrm{HV}) = 100.7 + 140.1/\sqrt{D(\mu\mathrm{m})} \quad (8)$$

In the available literature, the only available data for this alloy has been reported by Abdi et al. [3], which is related to the annealing at 1100 °C for 60 min after cold rolling. This data point is also includ-

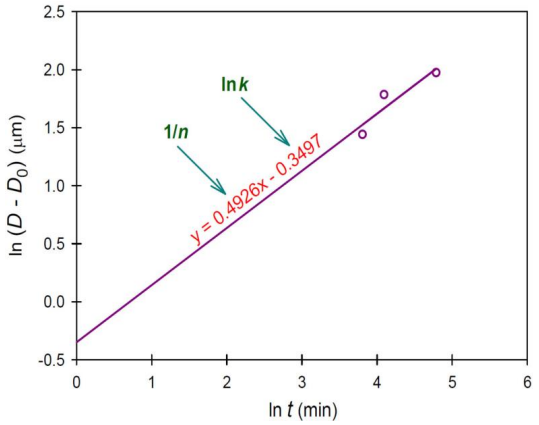

Fig. 4- Plot used to obtain the kinetic parameters of grain growth.

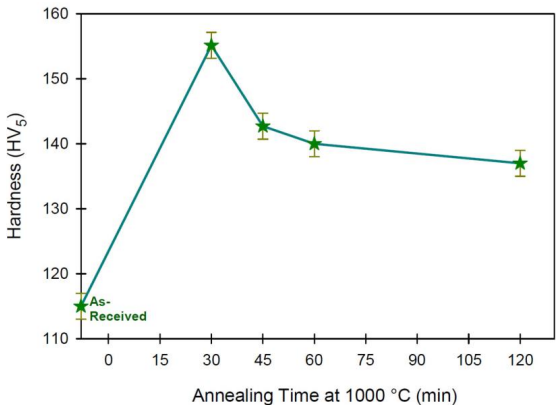

Fig. 5- Measured hardness of the annealed samples.

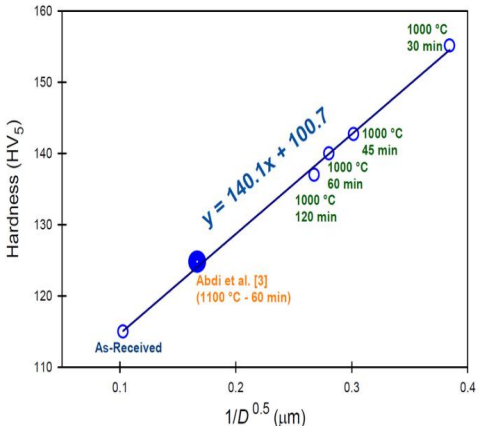

Fig. 6- Hall-Petch plot for the hardness of the AISI 309Si alloy.

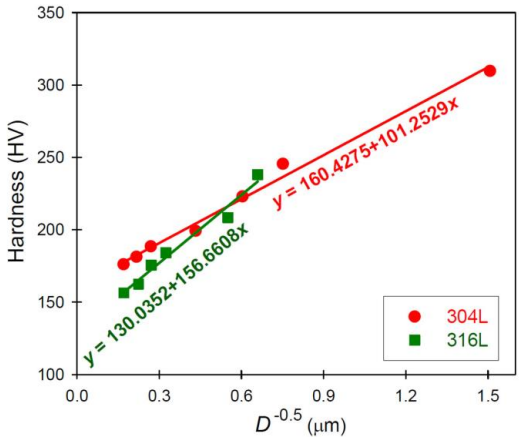

Fig. 7- Hall-Petch plots for AISI 304L and 316L stainless steels. The data are taken from [15], and the Hall-Petch analysis is performed in the present work.

ed in Figure 6, and it can be seen that it is consistent with the trend of data obtained in the present work. Therefore, it can be deduced that Equation 8 has captured the actual relationship between hardness and grain size in this alloy, which has been reported for the first time.

3.5. Comparison with other austenitic stainless steels

It seems that the H_0 value of 100.7 HV is quite low. To investigate the reason behind this observation, other commercial austenitic stainless steels, namely AISI 304L and 316L grades (Table 2), were also considered based on the hardness data reported in the work of Sohrabi et al. [15]. The data points were plotted in the form of a Hall-Petch plot in Figure 7.

Based on Figure 7, the values of H_0 for the AISI 304L and 316L can be determined as 160.4 and 130 HV, respectively. These values are much larger compared to the value of 100.7 HV for the AISI 309Si stainless steel. The main difference between these alloys is the difference in the metastability of the austenite phase, which can be assessed by the $M_{d30/50}$ temperature, which is the deformation temperature at which 50 vol% martensite forms at true tensile strain of 0.3 [29,30]:

$$M_{d30/50}(^{\circ}C) = 551 - 462(C+N) - 9.2Si - 8.1Mn - 13.7Cr - 29(Ni+Cu) - 18.5Mo - 68Nb - 1.42(Gs-8) \quad (9)$$

where Gs is the ASTM grain size number, and all the elements are expressed in weight percent. The obtained values of $M_{d30/50}$ temperature for the AISI 309Si, 304L, and 316L alloys were calculated by consideration of the chemical composition reported in Tables 1 and 2. Afterward, the dependency of H_0 on $M_{d30/50}$ temperature was investigated, as shown in Figure 8. It can be seen that the value of H_0 directly depends on the $M_{d30/50}$ temperature, and by increasing the $M_{d30/50}$ temperature (increasing the metastability of the alloy), the value of H_0 increases. This is related to the formation of more α′-martensite during indentation in the AISI 304L alloy compared to the AISI 309Si alloy, which leads to increased resistance to deformation and improved H_0.

4. Conclusions

In the present work, the Hall-Petch analysis of fine-grained AISI 309Si stainless steel upon recrystallization and grain growth annealing was investi-

Table 2-Chemical composition (wt.%) of the 304L and 316L alloys [15]

Alloy	C	Cr	Ni	Si	Mn	Cu	Mo	Fe
304L	0.01	18.6	8.3	0.38	1.4	0.11	0.1	balance
316L	0.01	17.3	10.1	0.46	1	0.38	2	balance

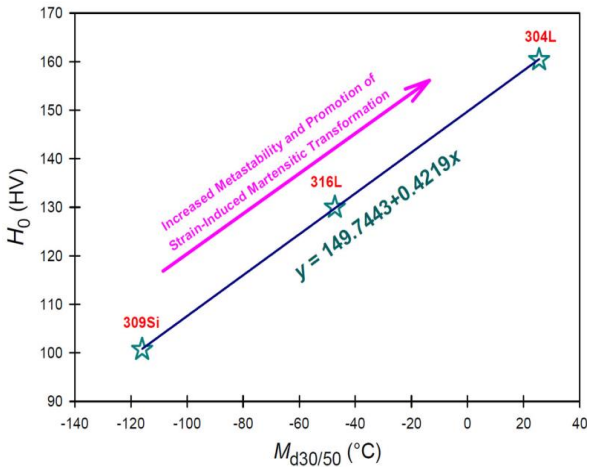

Fig. 8- Plot used to obtain the kinetic parameters of grain growth.

gated and compared with other commercial stainless steels. The following conclusions can be drawn:

(1) Cold rolling led to the formation of deformation-induced α′-martensite (~30 vol% martensite for 90% reduction in thickness) and work-hardening of the retained austenite, which led to an increased hardness of 427 HV compared to the hardness of 115 HV for the as-received sample.

(2) Annealing at 1000 °C for 30 min resulted in a significant increment of hardness (155.1 HV) compared to the as-received sample (115 HV) as well as the formation of a fine-grained microstructure with an average grain size of 6.7 μm compared to the as-received grain size of 95 μm, which is equivalent to ~93% refinement of the grain size.

(3) Annealing times longer than 30 min led to the occurrence of grain growth with the resulting decrement of hardness. Based on the parabolic grain growth analysis, the grain growth exponent of 2.03 was obtained, which is consistent with the theoretical value of 2. Moreover, to predict the grain size during grain coarsening, the equation of $D-D_0=2.1762\times10^{11}\exp(-280000/RT)\times t^{0.5}$ was proposed.

(4) The Hall–Petch relationship of $H=140.1/\sqrt{D}+100.7$ was proposed for the first time, in which the H_0 value of 100.7 HV was also compared to those determined for AISI 316L (130.0 HV) and 304L (160.4 HV) alloys. Furthermore, it was revealed that the increased metastability leads to an increment in the H_0 value, which can be correlated with the $M_{d30/50}$ temperature.

References

1. Eskandari M, Khosravi-Bigdeli I, Alavi Zaree SR, Yeganeh M. Effect of Cold-Rolling and Annealing Treatments on the Microstructure and Mechanical Properties of AISI 309S Austenitic Stainless Steel. Iranian Journal of Materials Forming. 2022 Jul 1;9(3):52-61.
2. Hsieh C-C, Lin D-Y, Chang T-C. Microstructural evolution during the δ/σ/γ phase transformation of the SUS 309LSi stainless steel after aging under various nitrogen atmospheric ratios. Materials Science and Engineering: A. 2008;475(1-2):128-35.
3. Abdi A, Mirzadeh H, Sohrabi MJ, Naghizadeh M. Phase Transformation Kinetics During Annealing of Cold-Rolled AISI 309Si Stainless Steel. Metallurgical and Materials Transactions A. 2020;51(5):1955-9.
4. Mohammadzehi S, Mirzadeh H. Cold unidirectional/cross-rolling of austenitic stainless steels: a review. Archives of Civil and Mechanical Engineering. 2022;22(3).
5. Belyakov A, Tikhonova M, Dolzhenko P, Sakai T, Kaibyshev R. On Kinetics of Grain Refinement and Strengthening by Dynamic Recrystallization. Advanced Engineering Materials. 2018;21(1).
6. El Wahabi M, Gavard L, Montheillet F, Cabrera JM, Prado JM. Effect of initial grain size on dynamic recrystallization in high purity austenitic stainless steels. Acta Materialia. 2005;53(17):4605-12.
7. Romero-Resendiz L, El-Tahawy M, Zhang T, Rossi MC, Marulanda-Cardona DM, Yang T, et al. Heterostructured stainless steel: Properties, current trends, and future perspectives. Materials Science and Engineering: R: Reports. 2022;150:100691.
8. Naghizadeh M, Mirzadeh H. Modeling the kinetics of deformation-induced martensitic transformation in AISI 316 metastable austenitic stainless steel. Vacuum. 2018;157:243-8.
9. Fultz B, Howe JM. Transmission Electron Microscopy and Diffractometry of Materials. Springer Berlin Heidelberg; 2001.
10. Etienne A, Radiguet B, Genevois C, Le Breton JM, Valiev R, Pareige P. Thermal stability of ultrafine-grained austenitic stainless steels. Materials Science and Engineering: A. 2010;527(21-22):5805-10.
11. Sohrabi MJ, Mirzadeh H, Sadeghpour S, Mahmudi R. Grain size dependent mechanical behavior and TRIP effect in a metastable austenitic stainless steel. International Journal of Plasticity. 2023;160:103502.
12. Zhou Z, Wang S, Li J, Li Y, Wu X, Zhu Y. Hardening after annealing in nanostructured 316L stainless steel. Nano Materials Science. 2020;2(1):80-2.
13. Geshani MS, Mirzadeh H, Sohrabi MJ. Detailed Hall–Petch Analysis of Cold Rolled and Annealed Duplex 2205 Stainless Steel. steel research international. 2022;93(7).
14. Lo KH, Shek CH, Lai JKL. Recent developments in stainless steels. Materials Science and Engineering: R: Reports. 2009;65(4-6):39-104.
15. Sohrabi MJ, Mirzadeh H, Dehghanian C. Significance of Martensite Reversion and Austenite Stability to the Mechanical Properties and Transformation-Induced Plasticity Effect of Austenitic Stainless Steels. Journal of Materials Engineering and Performance. 2020;29(5):3233-42.
16. Schramm RE, Reed RP. Stacking fault energies of seven commercial austenitic stainless steels. Metallurgical Transactions A. 1975;6(7):1345-51.
17. Shirdel M, Mirzadeh H, Parsa MH. Abnormal grain growth in AISI 304L stainless steel. Materials Characterization. 2014;97:11-7.
18. Järvenpää A, Jaskari M, Kisko A, Karjalainen P. Processing and Properties of Reversion-Treated Austenitic Stainless Steels. Metals. 2020;10(2):281.
19. Li J, Cao Y, Gao B, Li Y, Zhu Y. Superior strength and ductility of 316L stainless steel with heterogeneous lamella structure. Journal of Materials Science. 2018;53(14):10442-56.
20. Sun GS, Du LX, Hu J, Misra RDK. Microstructural evolution and recrystallization behavior of cold rolled austenitic stainless steel with dual phase microstructure during isothermal annealing. Materials Science and Engineering: A. 2018;709:254-64.
21. Kisko A, Hamada AS, Talonen J, Porter D, Karjalainen LP. Effects of reversion and recrystallization on microstructure and mechanical properties of Nb-alloyed low-Ni high-Mn austenitic stainless steels. Materials Science and Engineering: A. 2016;657:359-70.
22. Najafkhani F, Kheiri S, Pourbahari B, Mirzadeh H. Recent advances in the kinetics of normal/abnormal grain growth: a review. Archives of Civil and Mechanical Engineering. 2021;21(1).
23. Humphreys J, Rohrer GS, Rollett A. Recrystallization Textures. Recrystallization and Related Annealing Phenomena: Elsevier; 2017. p. 431-68.
24. Zamani MR, Mirzadeh H, Malekan M, Cao SC, Yeh J-W. Grain Growth in High-Entropy Alloys (HEAs): A Review. High Entropy Alloys & Materials. 2022;1(1):25-59.
25. Naghizadeh M, Mirzadeh H. Microstructural Evolutions During Reversion Annealing of Cold-Rolled AISI 316 Austenitic Stainless Steel. Metallurgical and Materials Transactions A. 2018;49(6):2248-56.
26. Forouzan F, Najafizadeh A, Kermanpur A, Hedayati A, Surkialiabad R. Production of nano/submicron grained AISI 304L stainless steel through the martensite reversion process. Materials Science and Engineering: A. 2010;527(27-28):7334-9.
27. Mehranpour MS, Heydarinia A, Emamy M, Mirzadeh H, Koushki A, Razi R. Enhanced mechanical properties of AZ91 magnesium alloy by inoculation and hot deformation. Materials Science and Engineering: A. 2021;802:140667.

28. Maleki M, Mirzadeh H, Zamani M. Effect of Intercritical Annealing Time at Pearlite Dissolution Finish Temperature (Ac1f) on Mechanical Properties of Low-Carbon Dual-Phase Steel. Journal of Materials Engineering and Performance. 2019;28(4):2178-83.
29. Nohara K, Ono Y, Ohashi N. Composition and Grain Size Dependencies of Strain-induced Martensitic Transformation in Metastable Austenitic Stainless Steels. Tetsu-to-Hagane. 1977;63(5):772-82.
30. Sohrabi MJ, Naghizadeh M, Mirzadeh H. Deformation-induced martensite in austenitic stainless steels: A review. Archives of Civil and Mechanical Engineering. 2020;20(4).